Available online at www.sciencedirect.com
SCIENCE DIRECT®
Journal of Luminescence 104 (2003) 151–158
JOURNAL OF LUMINESCENCE
www.elsevier.com/locate/jlumin

The effect of Cr concentration on emission cross-section and fluorescence lifetime in Cr,Yb:YAG crystal

Jun Dong[a,*], Peizhen Deng[b]

[a] School of Optics and Center for Research and Education in Optics and Lasers (CREOL), University of Central Florida, Orlando, FL 32816-2700, USA

[b] Shanghai Institute of Optics and Fine mechanics, Chinese Academy of Sciences, Shanghai 201800, People's Republic of China

Received 26 July 2002; received in revised form 2 January 2003; accepted 6 January 2003

Abstract

The emission cross-section, and fluorescence lifetime of Cr,Yb:YAG with different concentration of Cr^{4+} and Yb:YAG were measured. With the increase of Cr concentration in Cr,Yb:YAG, the emission cross-section keeps constant and fluorescence lifetime decreases. The quantum efficiency decreases and the energy transfer efficiency from Yb^{3+} to Cr^{4+} increase as the Cr concentration increases in Cr–Yb-co-doped Cr,Yb:YAG system. The nonradiative $Yb^{3+} \rightarrow Cr^{4+}$ energy transfer is consistent with an electric dipole–dipole interaction mechanism. The optimum Cr concentration for Cr,Yb:YAG was estimated. Also the potential of Cr,Yb:YAG as a self-Q-switched laser crystal was discussed.

Keywords: Cr,Yb:YAG crystal; Self-Q-switched; Energy transfer; Emission cross-section

1. Introduction

In recent years, Cr^{4+}-doped crystals have attracted a great deal of attention as passive Q-switches [1–4]. These Cr^{4+}-doped crystals include Cr^{4+}:YAG [1,2], Cr^{4+}:GSGG [3], Cr^{4+}:YSO [4], etc. They have a large absorption cross-section and low saturable intensity at the laser wavelength. In comparison with previously used saturable absorbers such as dyes [5] and LiF : F_2^- [6] color center crystals, Cr^{4+}-doped crystals are more photochemically and thermally stable and have a higher damage threshold. They can be used as Q-switches for both pulsed lasers [1,3,4] and continuously pumped lasers [2]. Moreover, Cr^{4+}:YAG can be co-doped with amplifying medium in a monolithic structure to form self-Q-switched laser [2]. As a result of the above mentioned advantages, Cr^{4+}-doped crystals become the most promising saturable absorbers for passively Q-switched lasers of stability, low cost, reliability, long life, compactness, and simplicity.

Recent advances in high performance strained layer diode lasers with wavelengths between 0.9 and 1.1 μm have stimulated interest in diode pumped Yb^{3+} laser [7,8]. Furthermore, because there are no additional 4f energy levels in Yb^{3+}

*Corresponding author. Tel.: +1-407-823-5009; fax: +1-407-823-6880.
E-mail address: jundong_99@yahoo.com, jundong@mail.ucf.edu (J. Dong).

0022-2313/03/$ - see front matter © 2003 Elsevier Science B.V. All rights reserved.
doi:10.1016/S0022-2313(03)00012-7

ions, as in other trivalent rare earths, complications in laser media which result from concentration quenching, up-conversion and excited state absorption are not anticipated to affect laser performance. At the same time, the broad emission band centered at 1.03 μm of Yb^{3+} couples well with the absorption of Cr^{4+}:YAG, and passively Q-switched Yb^{3+} lasers using Cr^{4+}:YAG as saturable absorber have been demonstrated [9–11]. Self-Q-switched Cr,Yb:YAG laser has also been demonstrated [12]. Compared to Nd ions in laser crystals, the Yb ion matches diode pumping ideally since it has a very simple energy level scheme with desirable properties for a laser system. The YAG crystal has a long storage lifetime (951 μs) [13] and a very low quantum defect (8.6%), resulting in three times less heat generation during lasing than comparable Nd-based laser systems [14]. In addition, the absorption at 940 nm makes this material highly suitable for diode pumping using InGaAs diodes which are potentially more robust than AlGaAs diodes used to excite Nd:YAG at 808 nm [8]. Another advantage of using Yb:YAG is that the 940 nm absorption feature is approximately five times broader than the 808 nm absorption feature in Nd:YAG and therefore the Yb:YAG system is less sensitive to diode wavelength specifications[15]. So Cr–Yb-co-doped Cr,Yb:YAG self-Q-switched laser crystal has the advantage over Cr,Nd:YAG, it will be a potential self-Q-switched laser material used for generating sub ns laser pulses.

In the present paper, we investigate the spectral parameters such as absorption coefficient, stimulated emission cross-section and fluorescence lifetime of Yb:YAG and different concentration Cr,Yb:YAG crystals. The concentration quenching effect of Cr,Yb:YAG crystals was observed with different Cr concentrations in Cr,Yb:YAG crystals. We explained these phenomenon using the energy transfer in Yb^{3+}–Cr^{4+} system, and study the dynamics of the excited state of Yb^{3+} ($^2F_{5/2}$) when energy transfer from Yb^{3+} to Cr^{4+} occurs. The study of the concentration quenching in Cr,Yb:YAG crystals will have great benefit to the development of the high quality, suitable Cr/Yb ratio Cr,Yb:YAG self-Q-switched laser crystals.

2. Experiments

Yb:YAG crystals doped with 10 at% Yb, Cr,Yb:YAG crystals co-doped with 10 at% Yb and 0.025 at%Cr, 0.1 at% Cr was grown by the Czochralski method. The detailed growth parameters are shown in Ref. [16]. Samples for spectroscopic and lifetime measurements were cut out of boules and the surfaces perpendicular to the ⟨1 1 1⟩ growth axis were polished. The thicknesses of the samples are 1 mm.

The absorption spectra were measured using a Cary 500 Scan UV–Vis–NIR spectrophotometer. Emission spectra were measured between 950 and 1100 nm. The excitation source was a diode laser operating at 943 nm. Yb^{3+} ions were pumped into their $^2F_{5/2}$ states and then relax nonradiatively to the ground $^2F_{7/2}$ state. The excitation signal was monitored during the experiment with a silicon (Si) detector. An indium gallium arsenide (InGaAs) detector located at the output slit of a 25 cm focal length Jarell-Ash monochromator was used to detect the fluorescence emission intensity. With 50-μm slits the resolution of this detection system was about 0.4 nm. Prior to use in calculating the stimulated emission cross-section, the recorded spectra were corrected for the spectral response of the detector and of the monochromator grating. The calibration of the detection system was achieved by recording its response to the light from a tungsten–iodine white light source that had been calibrated at the National Institute for Standards and Testing (NIST).

The excitation source for emission lifetime measurements was a single frequency (line width was 0.2 cm^{-1}), tunable optical parametric oscillator (Quanta Ray MOPO-SL) tuned to 941 nm. Its pulse duration was ~5 ns. The energy of the idler pulse delivered by the OPO at 941 nm is ⩽2 mJ. Fluorescence from the Cr,Yb:YAG and Yb:YAG samples was collected with a $f = 5$ cm lens and dispersed with the 25 cm focal length Jarell-Ash monochromator. An InGaAs photodiode connected to a preamplifier was used to detect the fluorescence emission intensity. Decay curves were recorded using a Tektronix 2440 500 Ms/s digital oscilloscope and computer controlled data acquisition system.

3. Results and discussion

The room temperature absorption spectra of Yb:YAG doped with 10 at% Yb^{3+} and Cr,Yb:YAG crystals co-doped with 10 at% Yb^{3+} and 0.1 at% and 0.025 at% Cr, respectively, are shown in Fig. 1a. With the increase of Cr concentration in Cr,Yb:YAG crystals, the absorption coefficient centered at 1.03 μm increases from 1.87 cm^{-1} for 10 at% Yb:YAG to 4.26 cm^{-1} for 0.1 at% Cr and 10 at% Yb-co-doped Cr,Yb:YAG. There is self-absorption at the lasing wavelength of 1.03 μm for Yb:YAG crystal; the absorption spectrum of Cr^{4+}, as shown in Fig. 1b, can be calculated by subtracting the absorption spectrum of 10 at% Yb:YAG from the absorption spectrum of Cr, Yb:YAG crystals, and the absorption coefficient of Cr^{4+} can also be calculated by subtracting the absorption coefficient of 10 at% Yb:YAG from the absorption coefficient of Cr,Yb:YAG at the lasing wavelength of 1.03 μm. Thus the absorption coefficients at 1.03 μm of Cr^{4+} in two different Cr,Yb:YAG crystal are 1.21 cm^{-1} for Cr,Yb:YAG crystal co-doped with 0.025 at% Cr and 10 at%

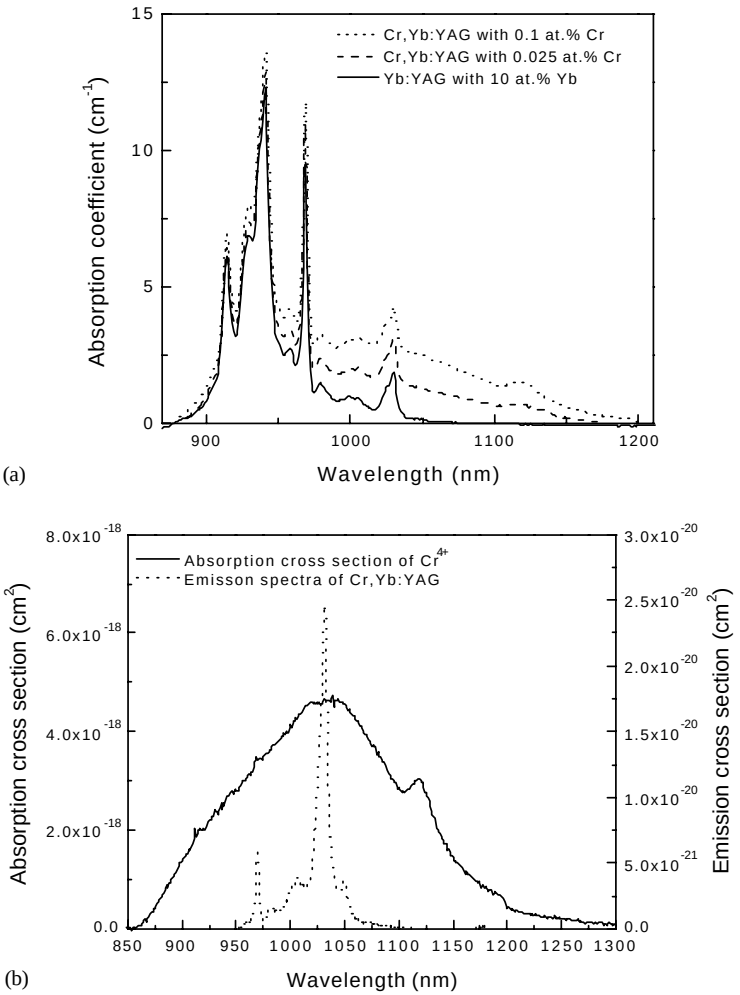

Fig. 1. (a) The absorption spectra of Yb:YAG and Cr,Yb:YAG crystals with different Cr concentration; (b) The absorption cross-sectional spectrum of Cr^{4+} in Cr,Yb:YAG crystals and the emission cross-sectional spectrum of Cr,Yb:YAG crystal at room temperature. The absorption spectrum covers the whole emission spectrum of Yb^{3+}, it is a suitable passively Q-switch for Yb^{3+} lasers.

Yb^{3+} and 2.40 cm^{-1} for Cr,Yb:YAG crystal co-doped with 0.1 at% Cr and 10 at% Yb^{3+}, respectively. From the Cr^{4+} absorption spectrum, the absorption cross-section of Cr^{4+} can be calculated (Cr^{4+} concentration can be estimated according to $[Cr^{4+}] \approx 0.04[Cr^{3+}]$ [17]), as shown in Fig. 1b, the broad absorption band is suitable for the passive Q-switch of rare earth doped solid-state lasers, the main absorption band is centered near 1.03 μm, is the ideal passive Q-switch for Yb^{3+} doped solid-state lasers. The absorption cross-section centered at 1.03 μm of Cr^{4+} of Cr,Yb:YAG crystal is about 4.68×10^{-18} cm^2, and the width of absorption band (FWHM) is about 200 nm.

The ytterbium emission from both YAG and Cr^{4+} co-doped YAG is not polarization dependent, so the emission spectra obtained could be used to calculate the effective stimulated emission cross-section of a Yb^{3+} ion from the manifold $^2F_{5/2} \rightarrow {}^2F_{7/2}$ transitions in the Yb:YAG and Cr–Yb-co-doped Cr,Yb:YAG by applying the Füchtbauer–Ladenburg formula. The fundamental relationship between spontaneous emission distribution $E_{(\lambda)} = I(\lambda)/\int I(\lambda)\mathrm{d}\lambda$ (integrating over all $^2F_{5/2} \rightarrow {}^2F_{7/2}$transitions) and the stimulated emission cross-section distribution $\sigma_{em}(\lambda)$[18] is

$$\sigma_{em}(\lambda) = \frac{1}{8\pi}\frac{\lambda^5}{n^2 c\tau}\frac{I(\lambda)}{\int I(\lambda)\lambda\,\mathrm{d}\lambda}, \quad (1)$$

where τ is the radiative lifetime of the upper laser level, c is the light velocity in vacuum, and n is the refractive index at the emission wavelength, the refractive index at 1030 nm is approximately 1.82. $I(\lambda)$ is the emission spectral intensity at different wavelength of Yb ions.

Fig. 2 shows the fluorescence spectra of Yb:YAG doped with 10 at% Yb^{3+} and Cr, Yb:YAG crystals co-doped with 10 at% Yb^{3+} and 0.1 at% and 0.025 at% Cr, respectively. The emission spectra of Yb:YAG and Cr,Yb:YAG crystals are nearly the same. There is a broad fluorescence spectrum from 955 to 1080 nm centered at 1.03 and 1.05 μm in Yb:YAG crystal. The strongest emission peak is centered at 1.03 μm and the emission cross-section calculated by F–L formula is 2.55×10^{-20} cm^2 for Yb:YAG, and the FWHM of the peak line width near 1.03 μm is about 9.0 nm. When Cr^{4+} ions were introduced into Yb:YAG crystals to form Cr–Yb-co-doped Cr,Yb:YAG crystals, the emission spectra of Cr,Yb:YAG crystals are nearly the same as that of Yb:YAG as shown in Fig. 2. The emission cross-section of Cr,Yb:YAG crystals is calculated to be 2.45×10^{-20} cm^2 by using F–L formula (the radiative lifetime of Yb^{3+} in YAG crystal is usually 951 μs [13]). So the emission spectral characteristics of Cr,Yb:YAG crystals keep the same as that of Yb:YAG crystal as the introduction of Cr^{4+} into Yb:YAG crystal.

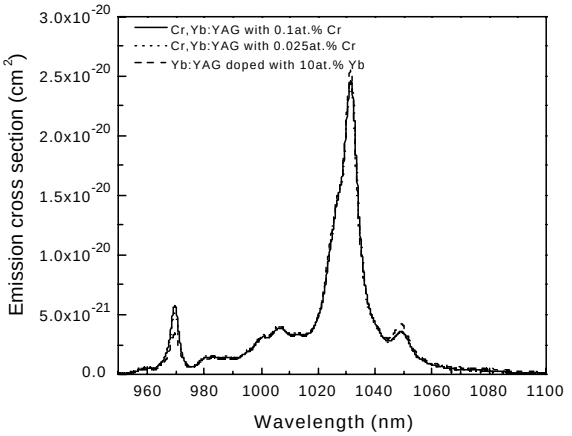

Fig. 2. Emission cross-sections of Yb:YAG and Cr,Yb:YAG crystals with different Cr concentrations.

The most predominant change of introducing of Cr^{4+} into Yb:YAG to form Cr,Yb:YAG crystals is the fluorescence lifetime, the fluorescence lifetime is shortened as Cr concentration increases. Fig. 3 shows the time-dependent behavior of the Yb^{3+} from the Yb:YAG crystal and Cr–Yb co-doped Cr,Yb:YAG crystals. The measured fluorescence lifetime of Yb:YAG crystal doped with 10 at% Yb^{3+} is 980 μs, which is in a good agreement, within experimental error, with the radiative lifetime of Yb:YAG (951 μs [13]). When Cr ions are introduced into Yb:YAG crystal to form Cr,Yb:YAG crystals, the fluorescence lifetime is shortened, 584 μs for 0.025 at% Cr and 360 μs for 0.1 at% Cr. The $^2F_{5/2} \rightarrow {}^2F_{7/2}$ Yb^{3+} emission occurs predominantly in the 955–1080 nm region and overlaps the broad absorption band $^3B_1(^3A_2) \rightarrow {}^3A_2(^3T_1)$ of Cr^{4+} (as shown in Fig. 1b), a requirement for efficient energy transfer. The Yb^{3+} fluorescence from

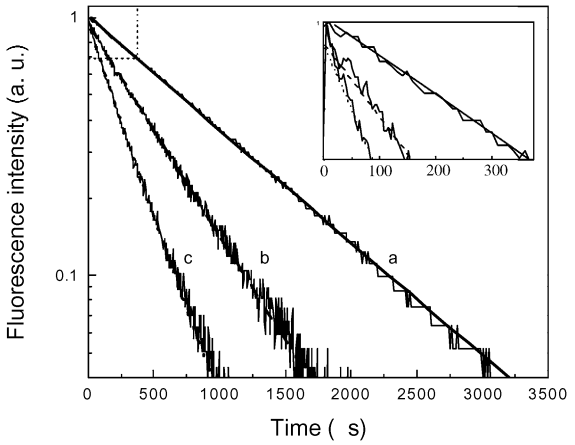

Fig. 3. Logarithmic plot of the fluorescence decays of the $2F_{5/2} \rightarrow 2F_{7/2}$ emission monitored at 1030 nm in the Cr,Yb:YAG crystals with different Cr concentrations, (a) 0 at% Cr, (b) 0.025 at% Cr, (c) 0.1 at% Cr, for an exaction wavelength of 941 nm measurements correspond to room temperature.

Yb:YAG crystal decays exponentially following pulsed excitation. When tetrahedral chromium ions are added, however, the decay initially deviates from a simple exponential dependence. This is illustrated in Fig. 3. The initial nonexponential portion of the decay is attributed to relaxation by direct $Yb^{3+} \rightarrow Cr^{4+}$ energy transfer. The final portion of the decay is exponential. Note that as the chromium concentration is decreased, the decay time of the exponential portion increases. This is characteristic of diffusion-limited relaxation since the average distance required for energy to migrate to a Cr^{4+} sink is increased. As the number of Cr^{4+} ions goes to zero, the total time dependence of the Yb^{3+} fluorescence decay approaches a single exponential with a lifetime given by the intrinsic decay time. When acceptor ions are present, donor ions in the vicinity of acceptors may interact with them via exchange or multipolar forces and transfer energy directly. According to the Inokuti–Hirayama model [19], if higher-order processes can be neglected, the normalized donor decay curves can be expressed by

$$\phi(t) = \exp\left[-\frac{t}{\tau_0} - \frac{4}{3}\pi\Gamma\left(1-\frac{3}{S}\right)N_a R_0^3\left(\frac{t}{\tau_0}\right)^{3/S}\right], \quad (2)$$

where $S = 6$, 8, and 10, respectively, for electric dipole–dipole, dipole–quadrupole, and quadrupole–quadrupole interactions. N_a is the acceptor concentration and R_0 is the critical transfer distance defined as the one for which the probability for energy transfer between a given donor–acceptor pair is equal to the donor intrinsic decay probability, τ_0^{-1}. R_0 can be found by fitting the initial portion of the decay curves in Fig. 3 to Eq. (2). For Cr,Yb:YAG crystal co-doped with 0.1 at% Cr and 10 at% Yb, again assuming dipole–dipole coupling, a value of $R_0 \approx 13.5$ Å was obtained. And $R_0 \approx 15.5$ Å was obtained for Cr,Yb:YAG crystal co-doped with 0.025 at% Cr and 10 at% Yb, also.

The lifetime of the $^2F_{5/2}$ state of an Yb^{3+} ion is governed by a sum of probabilities for several competing decay processes. These include (1) radiative decay, (2) nonradiative decay by multiphonon emission or self-quenching, and (3) energy transfer to Cr^{4+} or other impurities. Our measured fluorescence lifetime of Yb:YAG crystal (980 μs) is seen to approach the radiative lifetime (951 μs), hence the rate of nonradiative decay by multiphonon emission or self-quenching must by small in Yb:YAG crystal doped with 10 at% Yb^{3+}.

The energy transfer efficiency was calculated by the equation [20]

$$\eta = 1 - \tau/\tau_0, \quad (3)$$

where τ is the Yb^{3+} donor's lifetime for Yb^{3+} and Cr^{4+} co-doped Cr,Yb:YAG, and τ_0 is the radiative lifetime of Yb^{3+} in Yb:YAG crystal without other impurities.

And the quantum efficiency was calculated by the expression [21]

$$\eta_Q = \frac{\tau_f}{\tau_r}, \quad (4)$$

where τ_f is the measured fluorescence lifetime of Cr,Yb:YAG crystals, and τ_r is the radiative lifetime of Yb^{3+} in Cr,Yb:YAG crystals.

The variation of the energy transfer efficiencies from Yb^{3+} to Cr^{4+} and the quantum efficiencies with the concentration of Cr ions in Cr,Yb:YAG crystals is shown in Fig. 4. From Fig. 4, we can see that the quantum efficiencies reduces dramatically

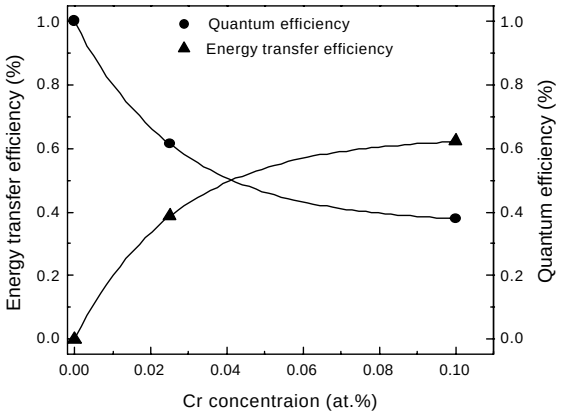

Fig. 4. Variation of quantum efficiency with the concentration of Cr ions and the energy transfer efficiencies from Yb^{3+} to Cr^{4+} in Cr,Yb:YAG crystals, the solid lines are used to illustrate the trend of the energy transfer efficiency and quantum efficiency.

with the increase of the concentration of Cr^{4+} in Cr,Yb:YAG crystals, the energy transfer efficiencies from Yb^{3+} to Cr^{4+} is very efficient. However, because of the strong luminescence quenching of Yb^{3+} as Cr concentration increases in Cr, Yb:YAG crystals, it is obvious that a compromise should be reached for maximizing the luminescence emitted by Yb^{3+} as a consequence of energy transfer from Yb^{3+} to Cr^{4+}. As the Cr^{4+} concentration increases in Cr,Yb:YAG crystals, the quantum efficiency of Yb^{3+} in Cr,Yb:YAG crystals reduces from unity for Yb:YAG crystal to 0.38 for Cr,Yb:YAG doped with 0.1 at% Cr, therefore, the concentration of Cr in Cr,Yb:YAG crystals has a great effect on the fluorescence lifetime and quantum efficiency. Also the energy transfer efficiency increases slowly with the increase of Cr concentration when Cr concentration reaches a certain value, so there is an optimum Cr concentration in Cr,Yb:YAG crystal to achieve high energy transfer efficiency and also keeps the quantum efficiency to a certain value. From Fig. 4, we can see that the optimum Cr concentration in Cr,Yb:YAG crystal should be 0.04 at%, at this value of Cr concentration, the quantum efficiency and energy transfer efficiency keep an optimum value, 50%.

Usually, there are two ways to realizing energy transfer in co-doped solid-state laser gain medium: direct energy transfer and energy migration to acceptors. The characteristics of donor system can be discussed in terms of three limiting cases [22]: (1) direct relaxation—no diffusion, (2) fast diffusion, and (3) diffusion-limited relaxation. When the acceptor concentration is low, as in Cr and Yb co-doped Cr,Yb:YAG crystal, only a small fraction of the total number of excited donors, Yb^{3+} are within the critical transfer distance of an acceptor, Cr^{4+}. Therefore, the donor decay will be governed principally by intrinsic relaxation and by diffusion-limited relaxation to acceptors. The decay of Cr,Yb:YAG crystal after the excitation pulse is described by an exponential function of time with a characteristic lifetime [22]

$$\frac{1}{\tau}=\frac{1}{\tau_0}+\frac{1}{\tau_D}, \tag{5}$$

where $1/\tau_D$ is the decay rate due to diffusion, τ is the fluorescence lifetime of Yb^{3+} in Cr,Yb:YAG crystal, τ_0 is the radiative lifetime of Yb^{3+} doped YAG crystal without other impurity ions. The solutions for τ_D have been obtained for the case where the donor–acceptor interaction arises from dipole–dipole coupling and is the form CR_0^{-6}, the resulting decay rate owing to diffusion between donors and acceptors is given by [22]

$$1/\tau_D = 8.5 N_a C^{1/4} D^{3/4}, \tag{6}$$

where N_a is the acceptor concentration, D is the diffusion constant between donor and acceptor, C is the constant defined as in following analysis.

The $Yb^{3+}\rightarrow Cr^{4+}$ energy transfer involves a pair of simultaneous energy-conserving transitions in which an excited Yb^{3+} ion decays from $^2F_{5/2}$ to a level of $^2F_{7/2}$ and a neighboring Cr^{4+} ion is excited from $^3B_1(^3A_2) \rightarrow {}^3A_2(^3T_1)$, as shown in Fig. 5. Although the exact multipolar or exchange nature of the $Yb^{3+}\rightarrow Cr^{4+}$ energy transfer process is uncertain, forced electric dipole–dipole transitions are possible for the two ions. We examine the transfer probability or dipole–dipole coupling given by [23].

$$W\left(Yb^{3+}-Cr^{4+}\right)=\frac{3h^4c^4\sum \mathrm{Cr}}{64\pi^5R^6n^4\tau_{Yb^{3+}}}K \times\int\frac{F_{Yb^{3+}}(E)F_{Cr^{4+}}(E)}{E}\,dE, \tag{7}$$

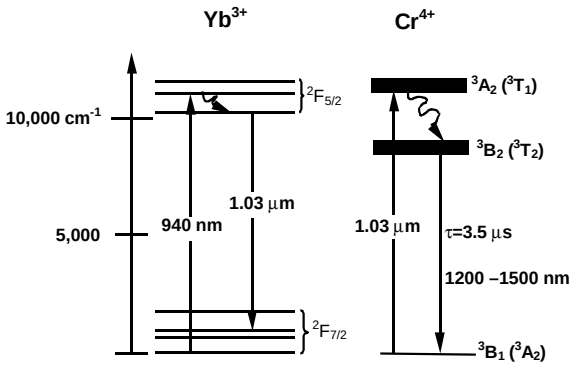

Fig. 5. Energy levels of Yb^{3+} and Cr^{4+} and relaxation mechanisms. τ, lifetime of the $^3B_2$ level.

where $\sum \mathrm{Cr} = \int \sigma(E)\mathrm{d}E$ is the integrated absorption cross-section of the acceptor ion Cr^{4+}, R is the separation of the Yb^{3+}–Cr^{4+} pair, $\tau_{Yb^{3+}}$ the radiative lifetime of Yb^{3+}, and K is a local correction factor of the material, which can be taken to be unity. In the spectral overlap integral $F_{Yb^{3+}}(E)$ and $F_{Cr^{4+}}(E)$are normalized line shape functions for the Yb^{3+} emission and Cr^{4+} absorption, respectively. The constant C was evaluated from Eq. (7) as

$$C = \frac{3h^4c^4 \sum \mathrm{Cr}}{64\pi^5 n^4} K \int \frac{F_{Yb^{3+}}(E) F_{Cr^{4+}}(E)}{E} \mathrm{d}E.$$

The overlap integral was determined from measurements of the Yb^{3+} fluorescence spectrum and the absorption spectrum for the Cr,Yb:YAG sample co-doped with 0.1 at% Cr and 10 at% Yb (as shown in Fig. 1b). The resulting value for C was about $6.88 \times 10^{-38}\,\mathrm{cm}^6/\mathrm{s}$.

According to the transfer probability for dipole–dipole coupling, Eq. (7), the critical transfer distance for dipole–dipole coupling is defined by

$$R_0 = (C\tau_0)^{1/6}, \quad (8)$$

where τ_0 is the radiative lifetime of Yb^{3+}. Using a value of $C = 6.88 \times 10^{-38}\,\mathrm{cm}^6/\mathrm{s}$ and a value of $\tau_0 = 951\,\mu\mathrm{s}$ yield $R_0 = 10.3\,\text{Å}$. In view of the assumptions made and experimental uncertainties, the agreement with the previous result for R_0 (calculated by using Eq. (2)) is considered satisfactory.

The diffusion constant can be evaluated from Eq. (6), while it is not sensitive to the value of C, it is dependent on the concentration of Cr^{4+} acceptors in Cr–Yb-co-doped Cr,Yb:YAG system. Using the nominal chromium concentrations and $C = 6.88 \times 10^{-38}\,\mathrm{cm}^6/\mathrm{s}$, a diffusion constant of $D \approx 6.21 \times 10^{-9}\,\mathrm{cm}^2/\mathrm{s}$ is obtained at room temperature.

The integral spectra between Yb^{3+} emission and Cr^{4+} absorption is very large (as shown in Fig. 1b), the energy can be transferred directly from Yb^{3+} ions to Cr^{4+} without the assistance of photon. Therefore, the influence of Cr^{4+} on the fluorescence lifetime of Cr,Yb:YAG is very significant. The energy transfer mechanism from Yb^{3+} ions to Cr^{4+} ions can be described as follows (Fig. 5): an excited Yb^{3+} ion decays from $^2F_{5/2}$ to a level of $^2F_{7/2}$ and simultaneously, a neighboring Cr^{4+} ion is excited from its ground state $^3B_1(^3A_2)$ to an intermediate state $^3A_2(^3T_1)$, because the $^3A_2(^3T_1)$ energy state is metastable and relax to the $^3B_2(^3T_2)$ level of Cr^{4+} ions very rapidly, the energy stored in the $^3B_2(^3T_2)$ level of Cr^{4+} ions is very stable compared to the decay from the $^3A_2(^3T_1)$ energy state to the $^3B_2(^3T_2)$ energy state of Cr^{4+}, the lifetime of the $^3B_2(^3T_2)$ energy state is about 3.5 μs and is very much shorter than the lifetime of the $^2F_{5/2}$ state of Yb^{3+} (about 980 μs), hence, Cr^{4+} serves as a fast-relaxing energy sink for Yb^{3+} excitation, and owing to the saturable absorption characteristics of Cr^{4+}, the absorption will increase with the increase of pump power until the saturable absorber, Cr^{4+}, reaches saturation (or "bleach"). When the saturable absorber, Cr^{4+}, is bleached, the energy stored in the cavity will be released instantly, so the high peak power pulses will be generated.

The independence of fluorescence spectra and the emission cross-section at 1.03 μm of Cr, Yb:YAG crystals with the increase of Cr concentration shows that the effective emission cross-section has not been changed with the introducing of Cr^{4+} ions in Cr,Yb:YAG. The decrease of the fluorescence lifetime of Cr,Yb:YAG crystals with the increase of Cr concentration shows that Cr^{4+} ions have the concentration quenching effect on the fluorescence of Yb^{3+} ions, and the quench

effect is strong as the Cr concentration increases. Therefore, the quantum efficiency of Cr,Yb:YAG decreases and the energy transfer efficiency increases as the Cr concentration increases. This is caused by the introduction of Cr ions during the growth of Cr, Yb co-doped Cr,Yb:YAG crystals, and the energy transfer from Yb^{3+} ions to Cr^{4+} is more efficiently. Compared to the Yb:YAG crystals, the fluorescence lifetime decreases and the emission cross-section keeps constant as the Cr concentration increases show that the saturation fluence of Cr,Yb:YAG will be higher than that of Yb:YAG, which makes Cr,Yb:YAG crystals suitable for using for self-oscillation of passively Q-switched oscillator.

4. Conclusion

The absorption spectra, fluorescence spectra and fluorescence lifetimes of Cr and Yb co-doped Cr,Yb:YAG crystals and Yb:YAG crystals were measured, with the increase of the Cr concentration in Cr,Yb:YAG crystals, the emission cross-sections of Cr,Yb:YAG keep constant and the fluorescence lifetimes decrease. The effective peak stimulated-emission cross-sections have been determined to be the same ($2.45 \times 10^{-20}\,cm^2$) for all the samples at room temperature. The luminescence lifetimes of Cr,Yb:YAG and Yb:YAG at room temperature are 360 μs for 0.1 at% Cr and 10 at% Yb co-doped Cr,Yb:YAG and 584 μs for 0.025 at% Cr and 10 at% Yb co-doped Cr,Yb:YAG, and 980 μs for 10 at% doped Yb:YAG , respectively. With the introduction of Cr in Cr,Yb:YAG crystals, the energy transfer efficiency increase dramatically, when the concentration of Cr approaches a certain value such as 0.06 at%, the energy transfer efficiency increases slowly, and the fluorescence lifetime decreases slowly, so the concentration of Cr in Cr,Yb:YAG has a optimum value 0.04 at% that will increase the energy transfer efficiency and keep the fluorescence lifetime and quantum efficiency to a suitable value for energy storage. This will make Cr,Yb:YAG crystal a more potential self-Q-switched laser material compared to Cr,Nd:YAG.

Acknowledgements

This work was supported by the National Natural Science Foundation of China under the project No. 6998806 and National 863-416 Foundation of China. The valuable comments of the unidentified reviewers also had a beneficial impact on the final manuscript.

References

[1] P. Yankov, J. Phys. D 27 (6) (1994) 1118.
[2] S. Zhou, K.K. Lee, Y.C. Chen, Opt. Lett. 18 (7) (1993) 511.
[3] W. Chen, K. Spariosu, R. Stultz, Opt. Commun. 104 (1) (1993) 71.
[4] Y.K. Kou, M.F. Huang, M. Birnbaum, IEEE J. Quantum Electron. 31 (4) (1995) 657.
[5] W. Kochner, Solid State Laser Engineering, 4th Edition, Springer, Berlin, Germany, 1992, pp. 489–493.
[6] J.A. Morris, C.R. Pollock, Opt. Lett. 15 (8) (1990) 440.
[7] D.P. Bour, D.B. Gilbert, K.B. Fabian, J.P. Bednarz, M. Ettenberg, IEEE Photon. Technol. Lett. 2 (1990) 173.
[8] S.L. Yellin, A.H. Shepard, R.J. Dalby, J.A. Baumaum, H.B. Serreze, T.S. Guide, R. Solarz, K.J. Bystrom, C.M. Harding, R.G. Walters, IEEE J Quantum Electron. 29 (1993) 2058.
[9] A.A. Lagatsky, A. Abdolvand, N.V. Kuleshov, Opt. Lett. 25 (9) (2000) 616.
[10] J. Dong, P. Deng, Y. Liu, Y. Zhang, J. Xu, W. Chen, X. Xie, Appl. Opt. 40 (24) (2001) 4303.
[11] Y. Kalisky, C. Labbe, K. Waichman, L. Kravchik, U. Rachum, P. Deng, J. Xu, J. Dong, W. Chen, Opt. Mater. 19 (4) (2002) 403.
[12] J. Dong, P. Deng, Y. Liu, Y. Zhang, G. Huang, F. Gan, Chin. Phys. Lett. 19 (3) (2002) 342.
[13] D.S. Sumida, T.Y. Fan, Opt. Lett. 19 (17) (1994) 1343.
[14] T.Y. Fan, IEEE J. Quantum Electron. 29 (6) (1993) 1457.
[15] H.W. Bruesselbach, D.S. Sumida, R.A. Reeder, R.W. Byren, IEEE J. Selected Topics Quantum Electron. 3 (1) (1997) 105.
[16] J. Dong, P. Deng, J. Xu, J. Cryst. Growth 203 (1999) 163.
[17] A.G. Okhrimchuk, A.V. Shestakov, Opt. Mater. 3 (1994) 1.
[18] P. Haumesser, R. Gaume, B. Viana, D. Vivien, J. Opt. Soc. Am. B19 (10) (2002) 2365.
[19] M. Inokuti, F. Hirayama, J. Chem. Phys. 43 (1965) 1978.
[20] R. Reisfeld, Y. Kalisky, Chem. Phys. Lett. 80 (1) (1981) 178.
[21] H.D. Jiang, J.Y. Wang, H.J. Zhang, X.B. Hu, H. Liu, J. Appl. Phys. 92 (2002) 3647.
[22] M.J. Weber, Phys. Rev. B 4 (9) (1971) 2932.
[23] D.L. Dexter, J. Chem. Phys 21 (5) (1953) 836.